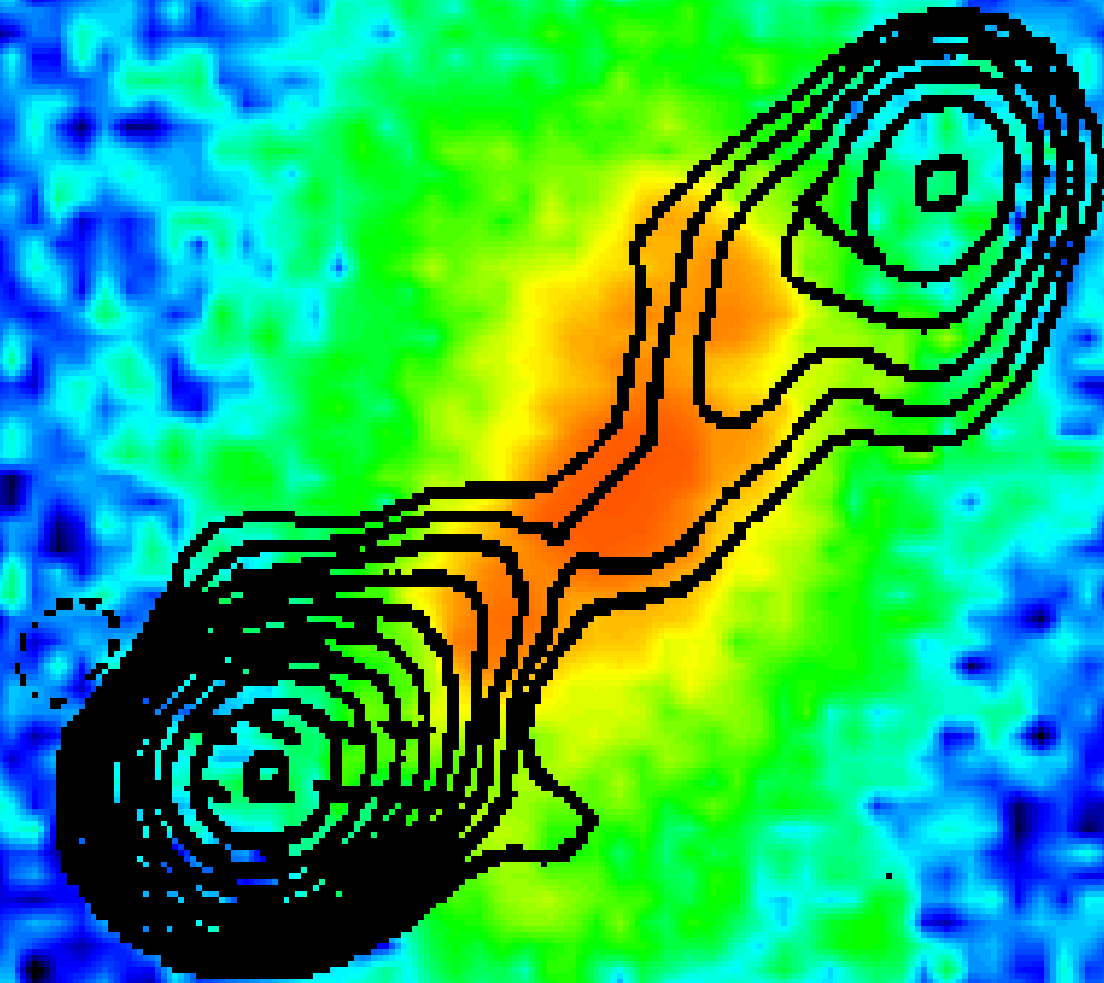


Lecture 3: Young radio galaxies

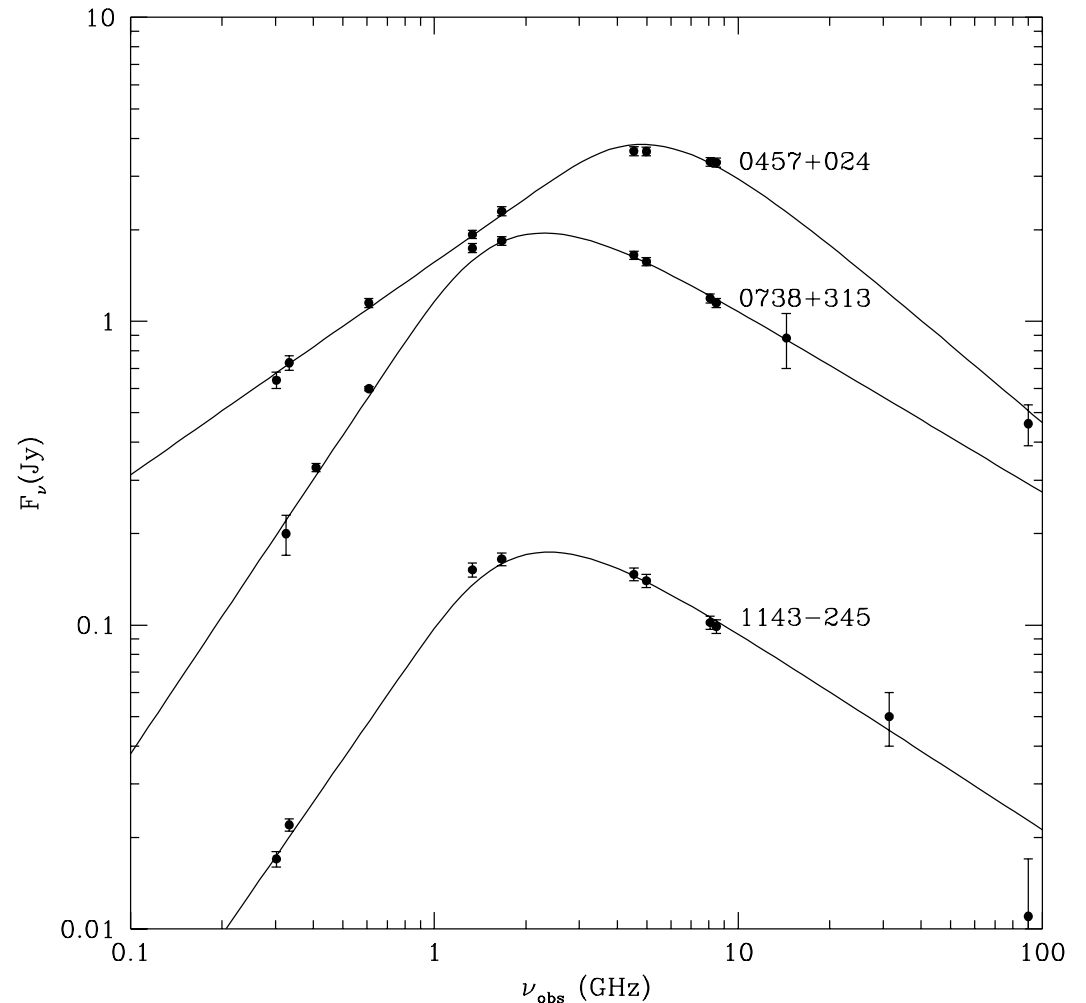


Geoff Bicknell RSAA, ANU

1 Gigahertz Peak Spectrum and Compact Steep Spectrum Sources

GPS = Gigahertz Peak Spectrum - characterised by a peak in the radio spectrum at ~ 1 GHz

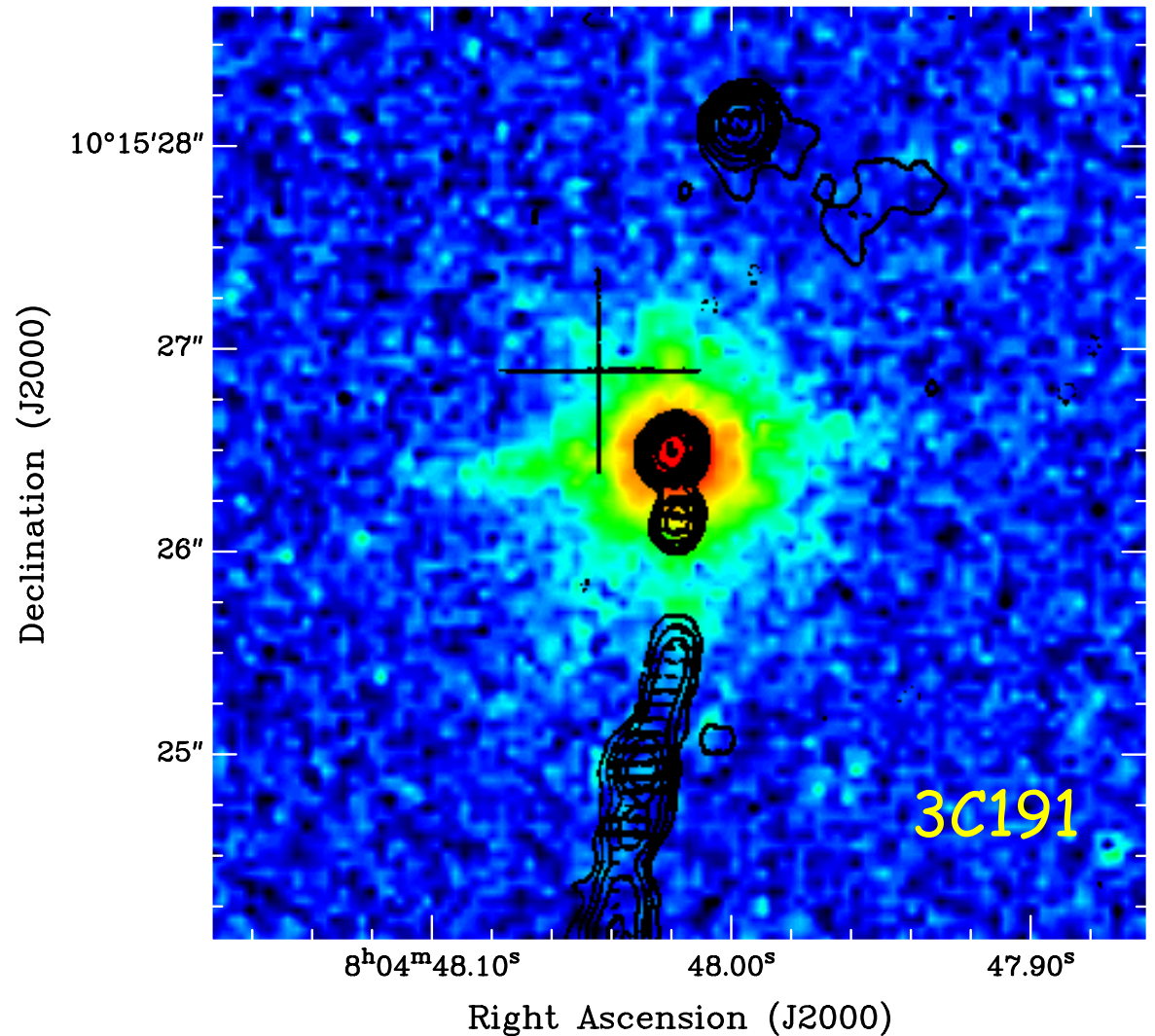
CSS = Compact Steep Spectrum - have steep spectra at microwave frequencies but also have a peak in the spectrum in the 10-100 MHz range



CSS examples

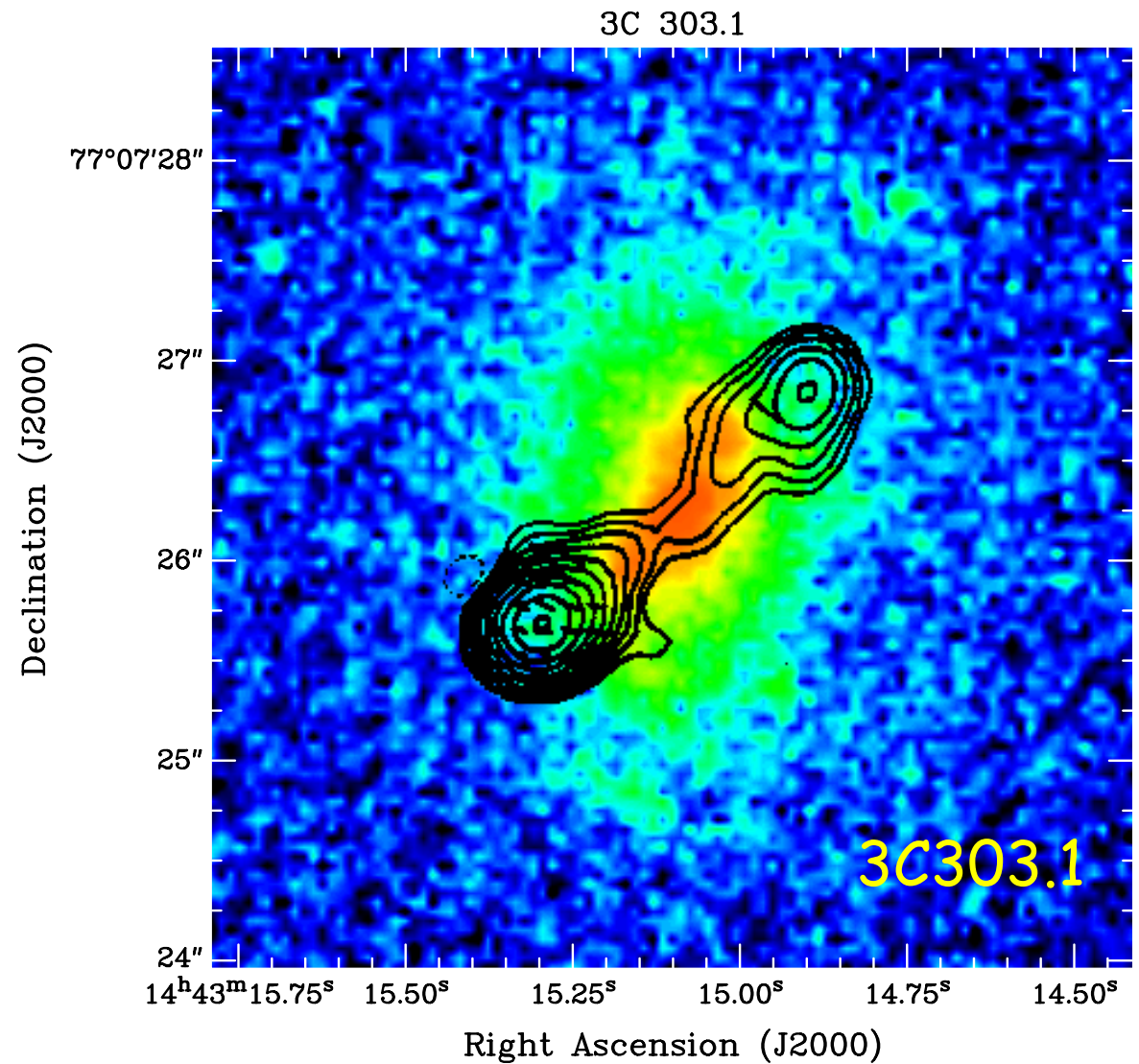
The image on the right from de Vries et al (1997, ApJS, 110, 191) shows the CSS quasar, 3C191 superposed on an HST optical image

The radio source is a few arcseconds ~ 5 -10 kpc in extent



3C 303.1 is a galaxy at $z = 0.270$

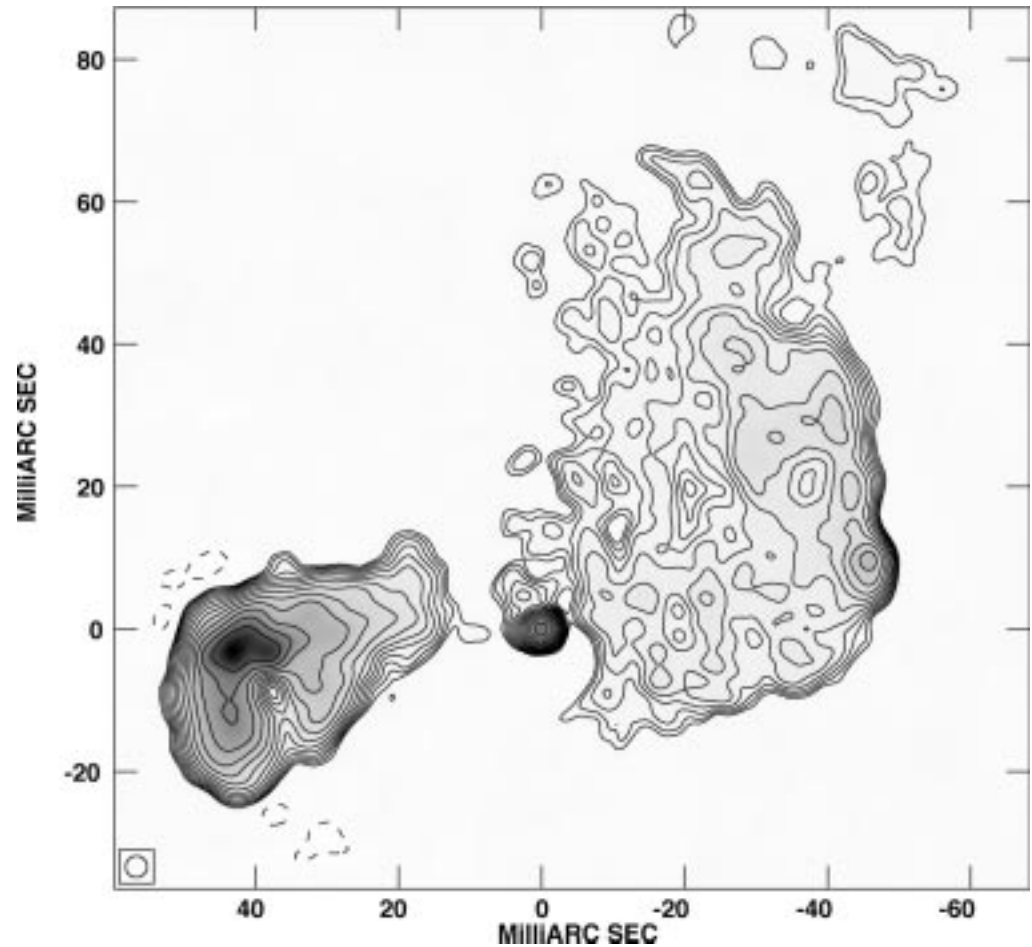
The optical emission from the orange-green region is dominated by emission lines from dense ($n \sim 10 - 100 \text{ cm}^{-3}$) gas clouds



GPS example

4C 31.05 is a GPS source.

In this case the angular scale
 $\sim 0.1''$ and the source is of or-
der 500 pc in size

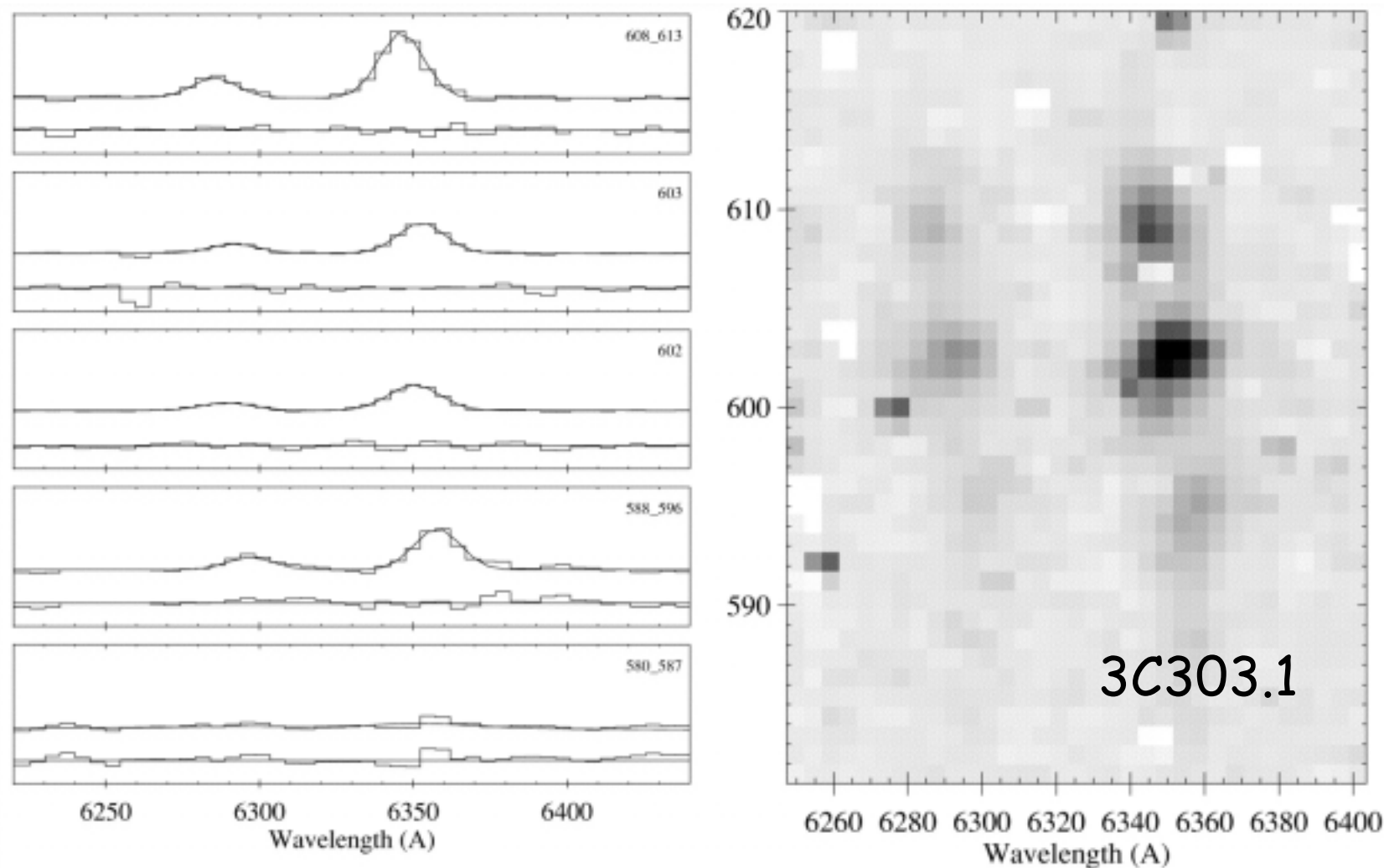


Measured advance speeds

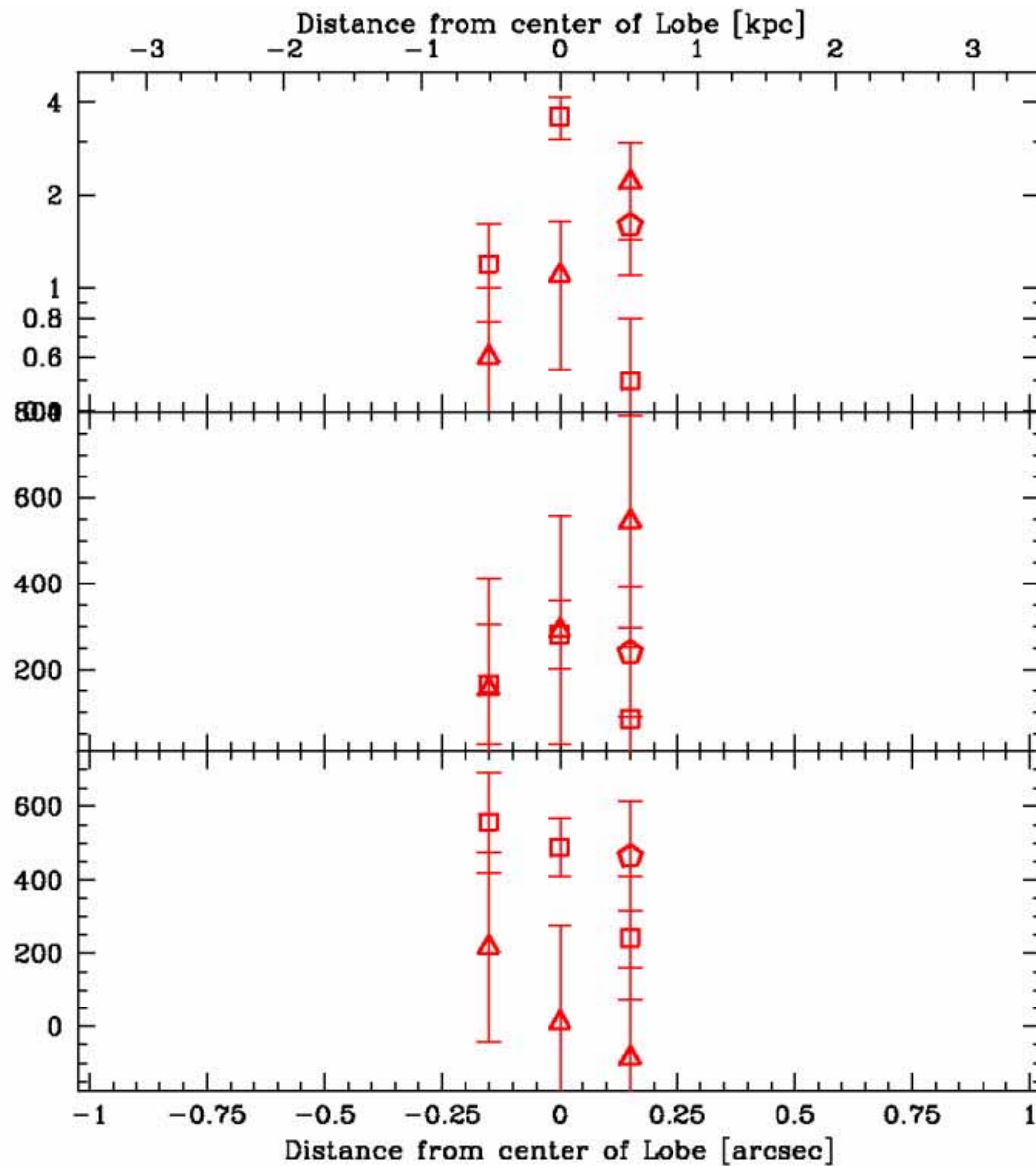
- GPS $\sim 0.1 - 0.4 c$ (Conway, Murgia et al.)
- CSS $\sim 0.05 - 0.1 c$

2 Physical picture of GPS and CSS sources

Spectra (O'Dea, deVries et al., 2002, AJ, 123, 2333)



Kinematics of gas



- Radio-emission line alignment => shock excitation of emission lines

- Velocity offsets from systemic $\sim 100 - 500 \text{ km s}^{-1}$

- Broad $\sim 100 - 500 \text{ km s}^{-1}$ profiles and split lines

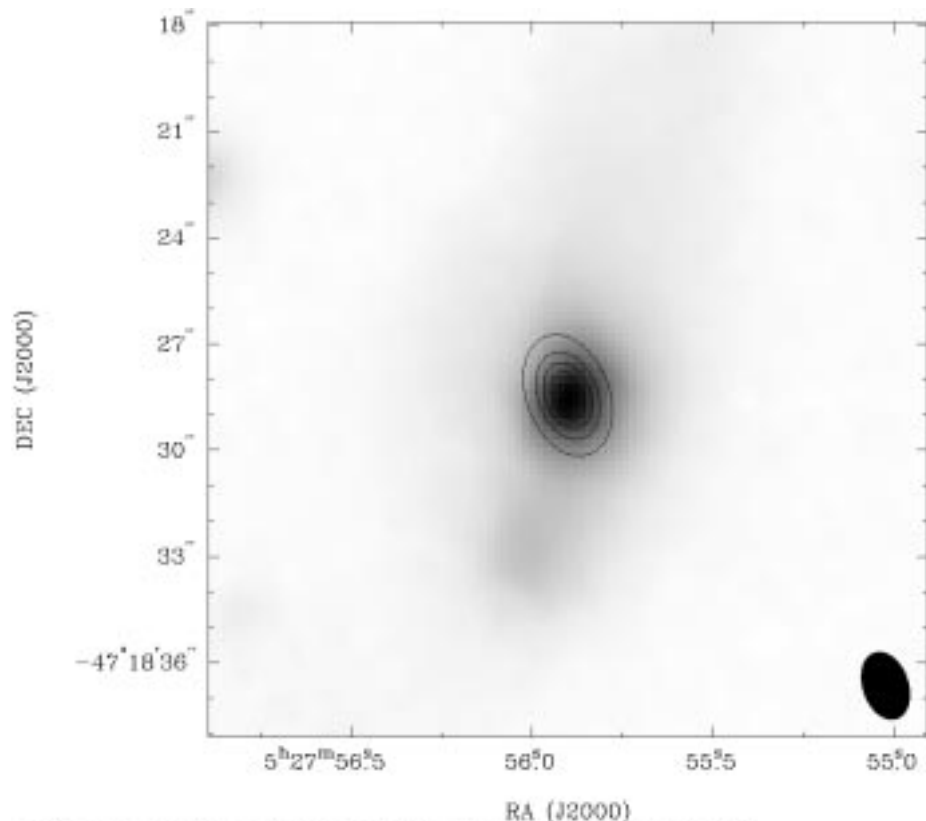
Notional model (See Kawakatu, Umemura and Mori, ApJ, 2003, 583, 85)

- Development of cosmological large scale structure => regions of high density => mergers
- Merger => Ultra Luminous InfraRed Galaxy
- Some of the resulting merger debris cleared away by winds from the resulting starburst
- System settles down to a steady accretion flow => Gas is accreted onto the central black hole => Radio source

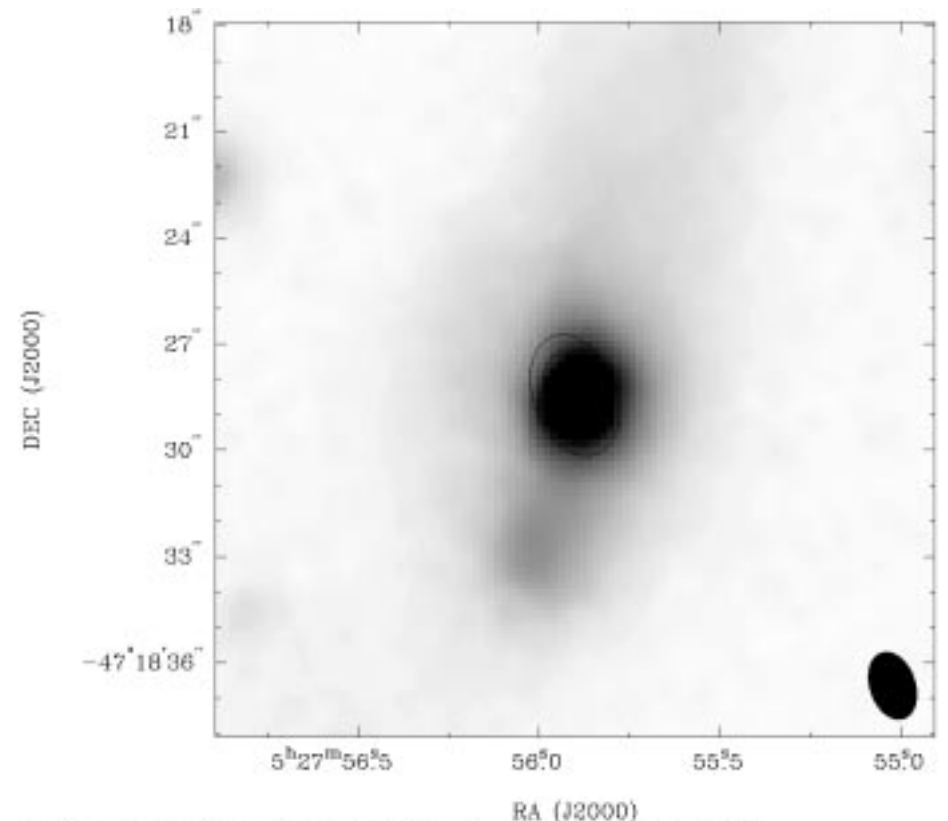
Related point: Radio galaxies and cosmology

Densest regions in the universe seem to be indicated by powerful radio galaxies

3 CSS galaxy sample (Drake, McGregor)



RA, DEC, FREQ = 5:27:55.901, -47:18:45.01, 8.83994759E+08 GHz at pixel (513.00, 513.00, 1.00)
Spatial region : 483,563 to 563,663
Pixel map image: /data/magellan/odrake/c532/overlay/image.tmp (F052M5-4720) Min/max=4224/1.4647e10 Range
Contour image: /data/magellan/odrake/c539/maps/156346-4720.6640.cmap Min/max=-1.495e-10/0.1413 Contours
Contours : 10, 30, 50, 70, 90, 90



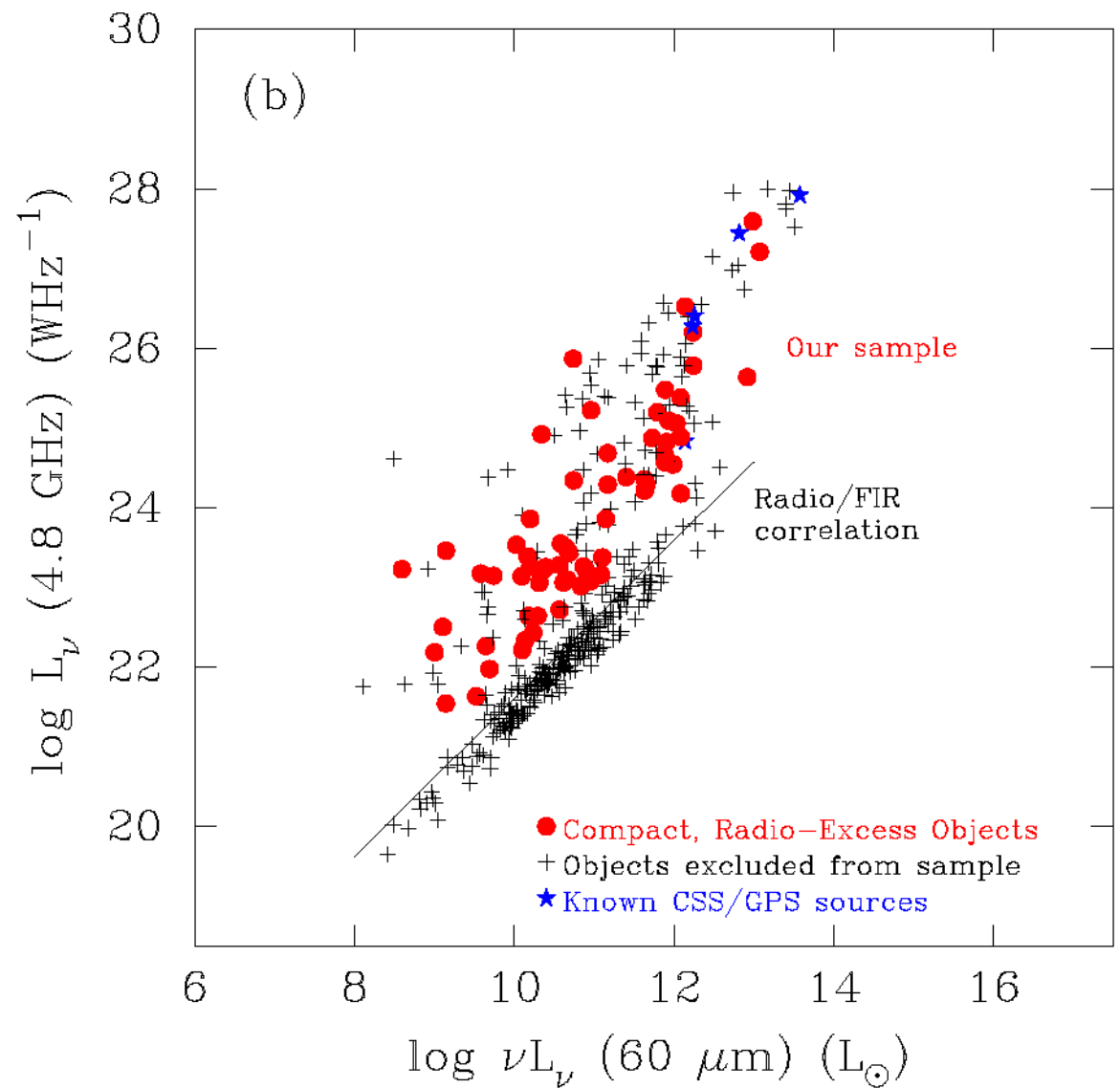
RA, DEC, FREQ = 5:27:55.901, -47:18:45.01, 8.83994759E+08 GHz at pixel (513.00, 513.00, 1.00)
Spatial region : 483,563 to 563,663
Pixel map image: /data/magellan/odrake/c532/overlay/image.tmp (F052M5-4720) Min/max=4224/1.4647e10 Range
Contour image: /data/magellan/odrake/c539/maps/156346-4720.6640.cmap Min/max=-1.495e-10/0.1413 Contours
Contours : 10, 30, 50, 70, 90, 90

Cross-correlation of Parkes-MIT-NRAO survey and IRAS catalogue => Number of examples of unresolved-barely resolved radio sources coincident with merging galaxies

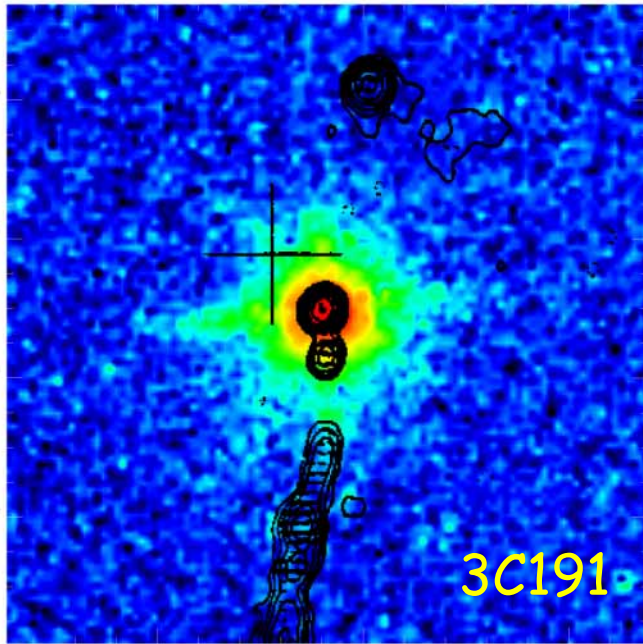
Radio - IR relation

Normal galaxies show a correlation between radio and Far IR emission that may be related to the connection between cosmic rays and star formation

Active galaxies show an excess of radio emission



4 Radiative jet-ISM interactions in young radio sources (Bicknell, Saxton & Sutherland)



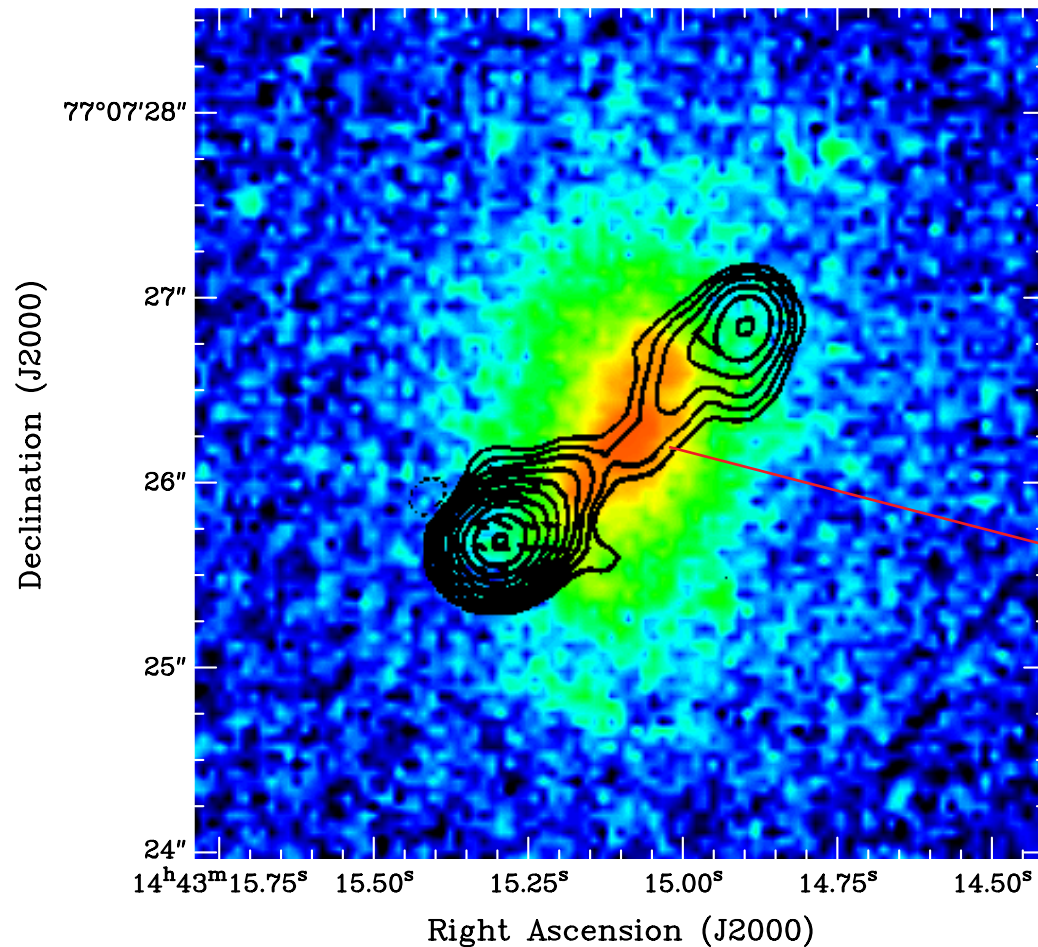
Expansion velocity

- Measured advance speeds $\sim 0.1 - 0.4 c$ (Conway 2002, Murgia et al. 1999 etc.)
- Consistent with self-similar model (Begelman, 1996; Bicknell, Dopita & O'Dea, 1997, ApJ, **485**, 112):

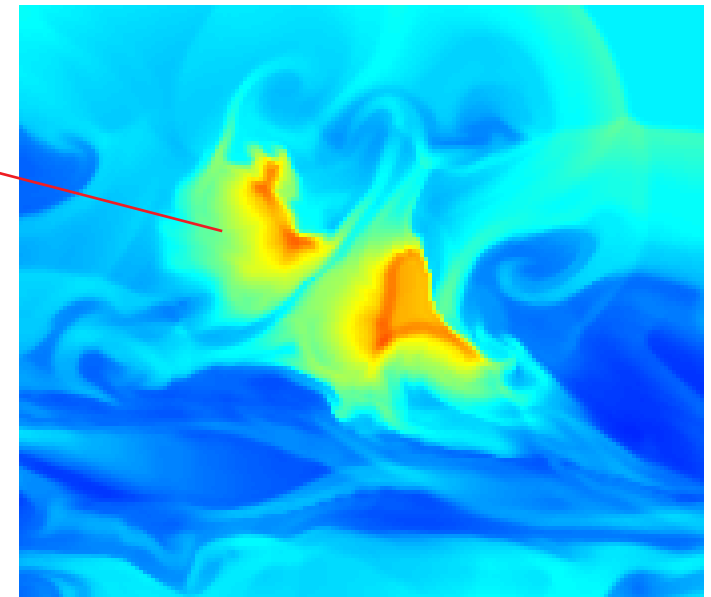
$$\frac{v_b}{c} \approx 0.056 \left[\frac{F_{E, 46}}{(n_H(\text{kpc})) / (0.01 \text{ cm}^{-3}))} \right]^{1/3} \left[\frac{R}{\text{kpc}} \right]^{\frac{\delta - 2}{3}}$$

Parameters of shocked emission line clouds

- Shocks driven into clouds by over-pressure of cocoon:



$$SB([OIII]) \approx 2.3 \times 10^{-2} \times \text{Cov. Factor} \\ \times n_H \left(\frac{v_{sh}}{10^3 \text{ km s}^{-1}} \right)^3 \text{ ergs cm}^{-2} \text{ s}^{-1}$$

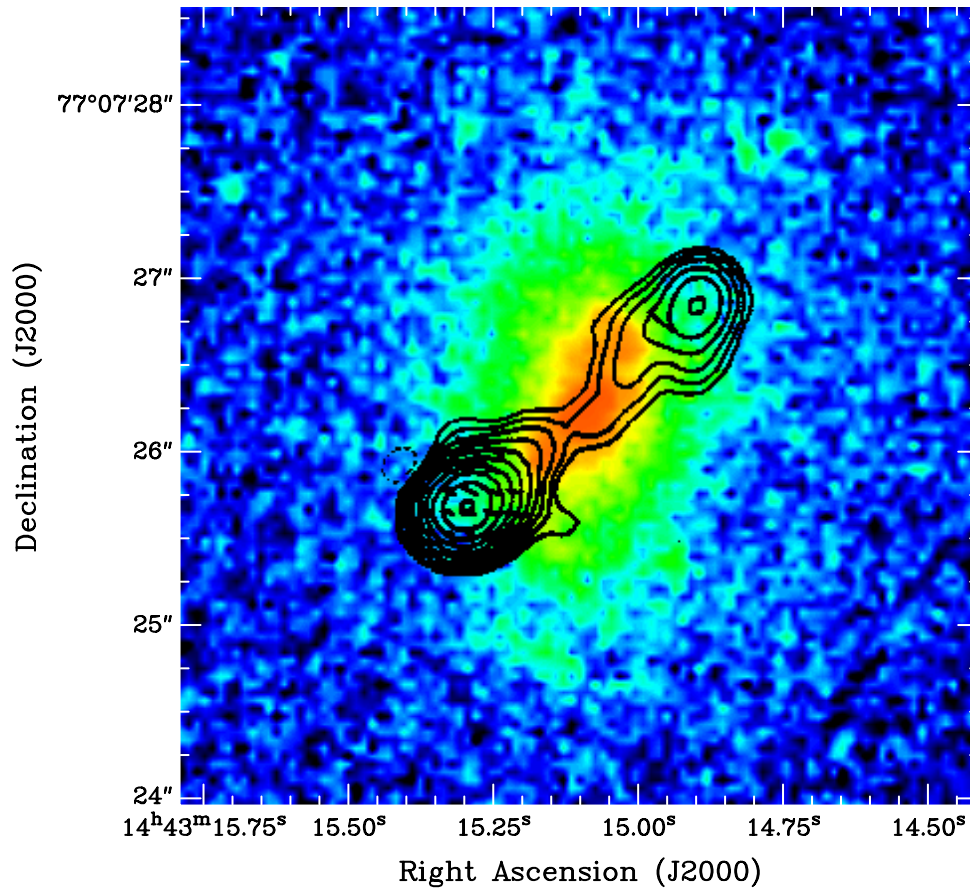


$$v_{sh} \approx 300 \left(\frac{n_{cl}/n_{ism}}{10^4} \right)^{-1/2} \left(\frac{v_b}{0.1c} \right) \text{ km s}^{-1}$$

- Shocks take a finite time to become fully radiative => not all shocked clouds give an optical spectrum
- Radiative time scale less than dynamical time scale (GB, Saxton & Sutherland, 2002) requires:

$$\frac{v_b}{c} < 0.024 n_{cl}^{0.2} \left(\frac{n_{cl}/n_{ism}}{10^4} \right)^{0.4} \left(\frac{R}{5 \text{ kpc}} \right)^{0.2}$$

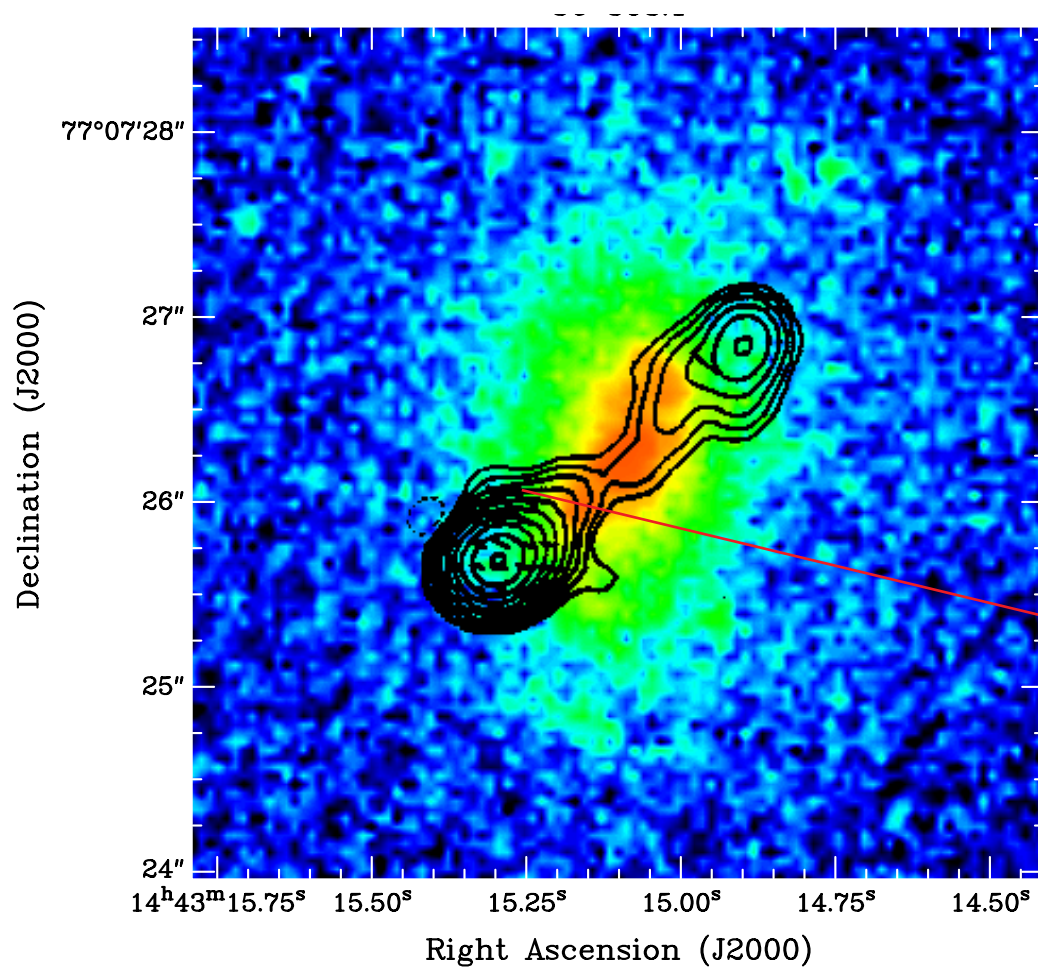
- Marginally consistent with estimated advance speeds
- May be valid at sides of bow shock if not at apex



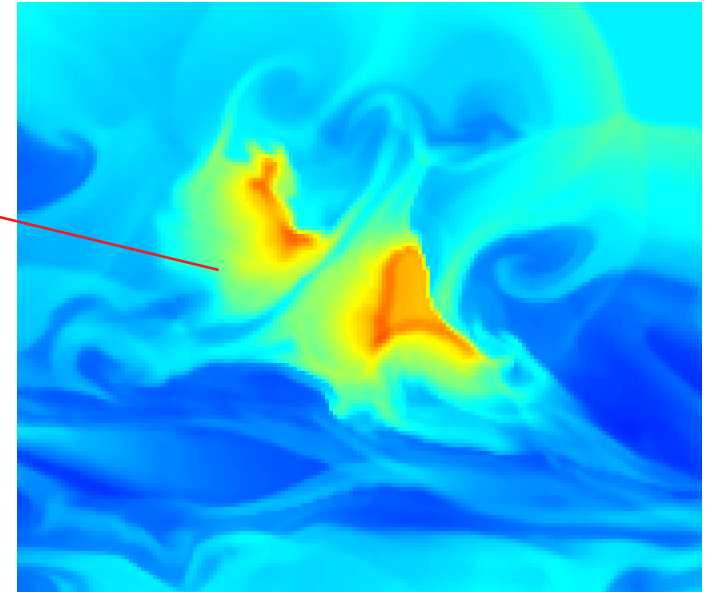
Two possibilities for trailing optical emission:

- Bow-shock non-radiative near apex
- Limited spatial extent of dense clouds

Emission line surface brightness



$$SB([OIII]) \approx 2.3 \times 10^{-2} \times \text{Cov. Factor} \\ \times n_H \left(\frac{v_{sh}}{10^3 \text{ km s}^{-1}} \right)^3 \text{ ergs cm}^{-2} \text{ s}^{-1}$$



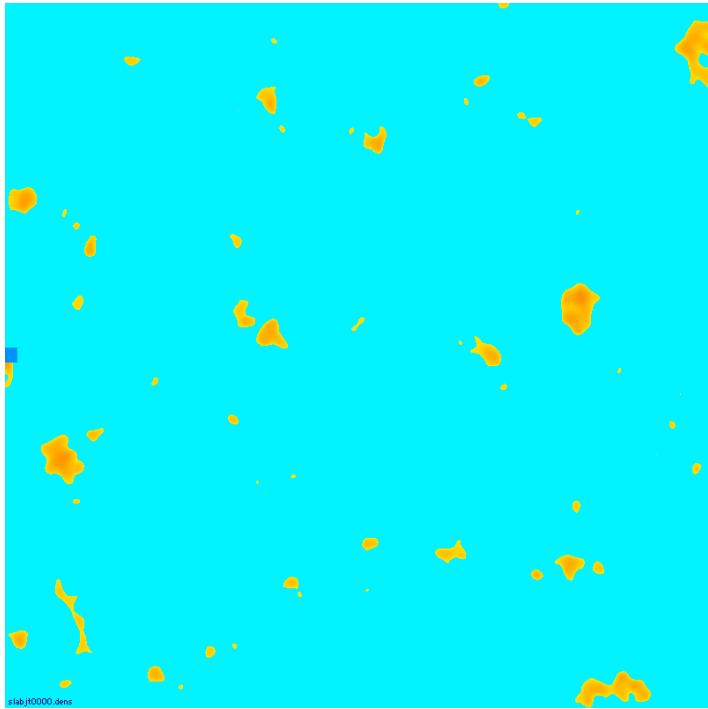
Estimates of parameters

Use:

- [OIII] surface brightness and bow-shock expansion speeds (de Vries et al. 1997)
- velocity widths - related to shock speeds and density

Source	Expansion speed	n_H (cm^{-3})	Covering factor
<i>3C277.1</i>	<i>0.04 c</i>	<i>6</i>	<i>33</i>
<i>3C303.1</i>	<i>0.07 c</i>	<i>14</i>	<i>3</i>

5 Slab jet simulations of radio plasma-cloud interactions



Features:

- Distributions of clouds generated in Fourier space => randomly placed and shaped clouds

- $k_{max} = \frac{2\pi}{4} \text{ pixels}$

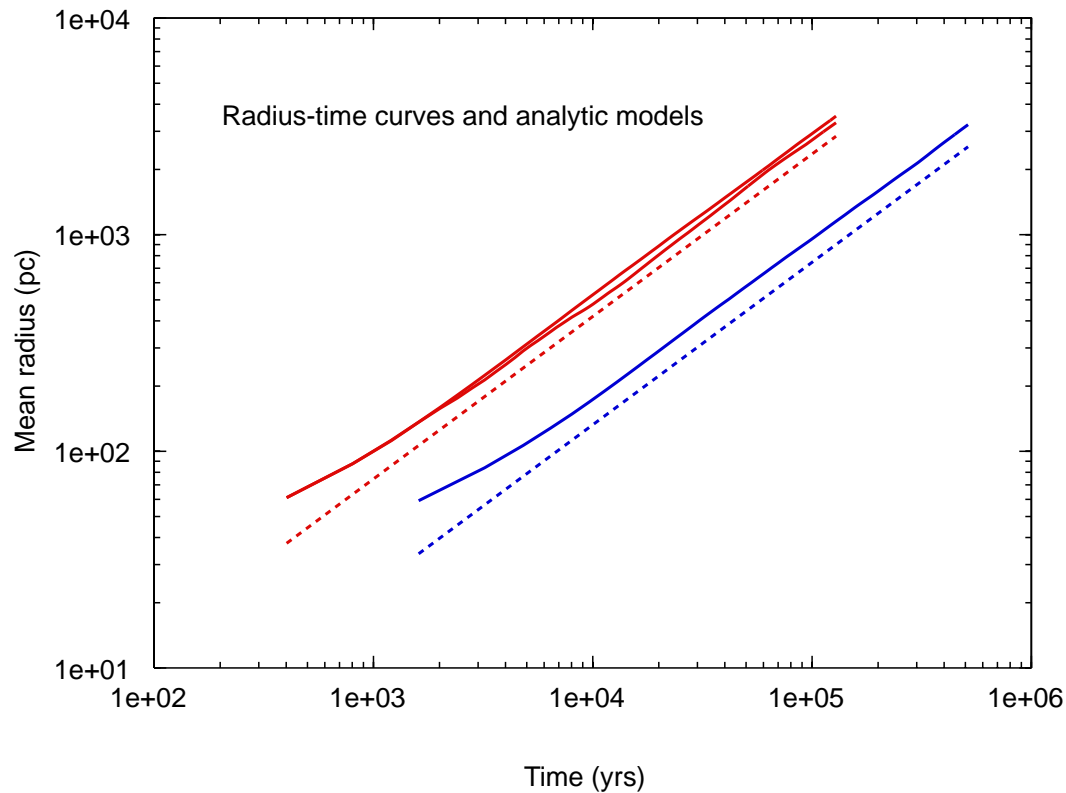
- $k_{min} = k_{Jeans}$

- In later simulations, no clouds within Roche limit of 10^8 solar mass black hole

Simulation parameters

Sim	$\frac{p_{jet}}{p_{ism}}$	η	M	r_{jet} (pc)	$F_{E, 46}$ (equiv)	Grid (kpc)	n_{ism}	$\frac{n_{cl}}{n_{ism}}$
<i>slab02</i>	<i>130</i>	<i>0.38</i>	<i>35</i>	<i>25</i>	<i>0.03</i>	<i>1.9</i>	<i>0.01</i>	<i>10³</i>
<i>slab09/ erupt01</i>	<i>1</i>	<i>1.1×10⁻³</i>	<i>127</i>	<i>10</i>	<i>1.0</i>	<i>1.6</i>	<i>1</i>	<i>10³</i>
<i>slab11/ erupt02</i>	<i>1</i>	<i>1.1×10⁻³</i>	<i>127</i>	<i>10</i>	<i>1.0</i>	<i>1.6</i>	<i>1</i>	<i>10³</i>

6 Comparison with 2D energy driven bubble



Radius of 2D energy driven bubble:

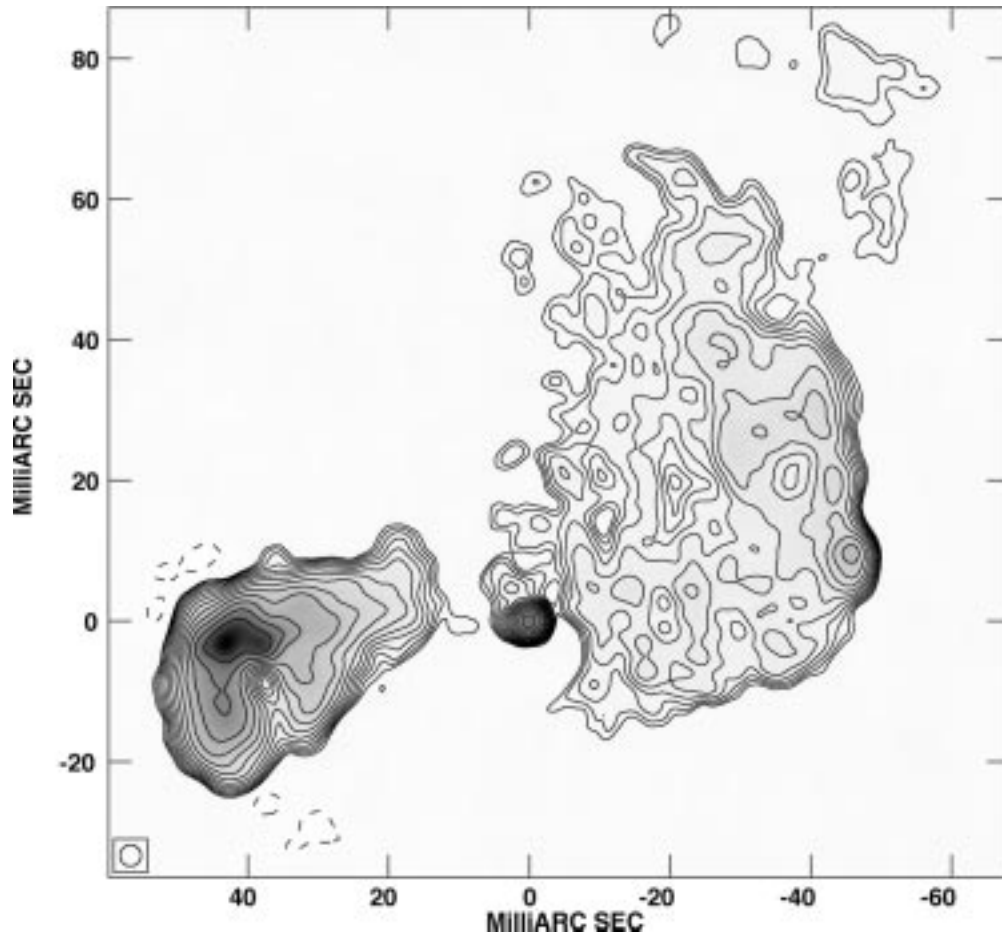
$$R = \left[\frac{4A}{9\pi\rho_0} \right]^{1/4} t^{3/4}$$

$A =$ Energy flux
per unit length

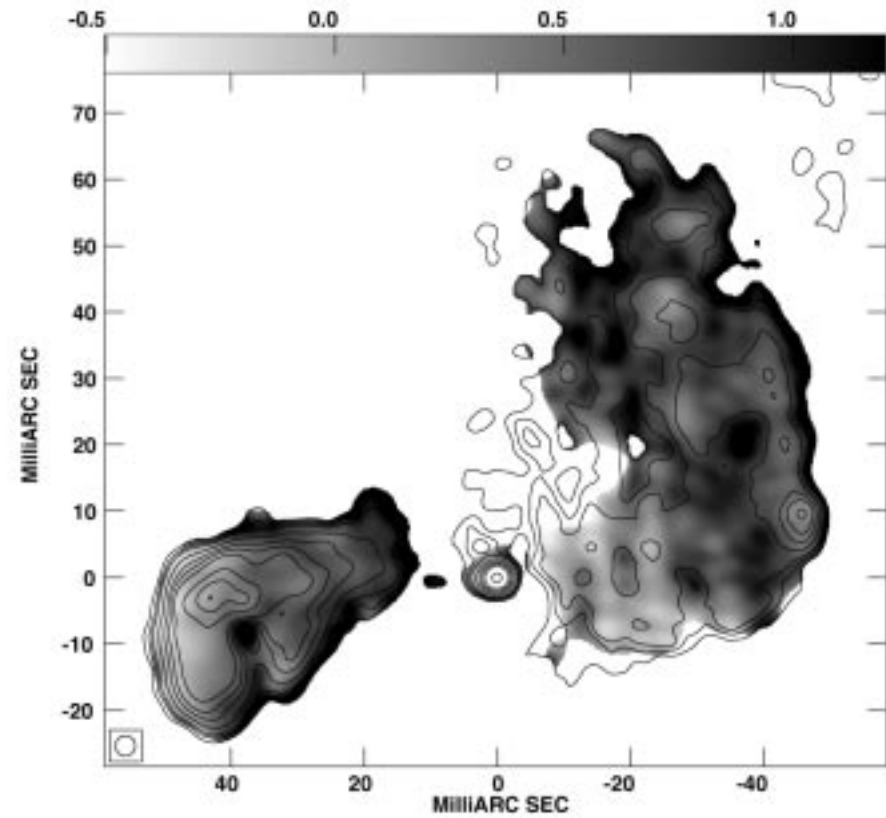
Intermediate stage in 3D should also be energy-driven bubble

$$R \propto t^{3/5}$$

7 Comparison with 4C31.05 (Giovannini et al.)

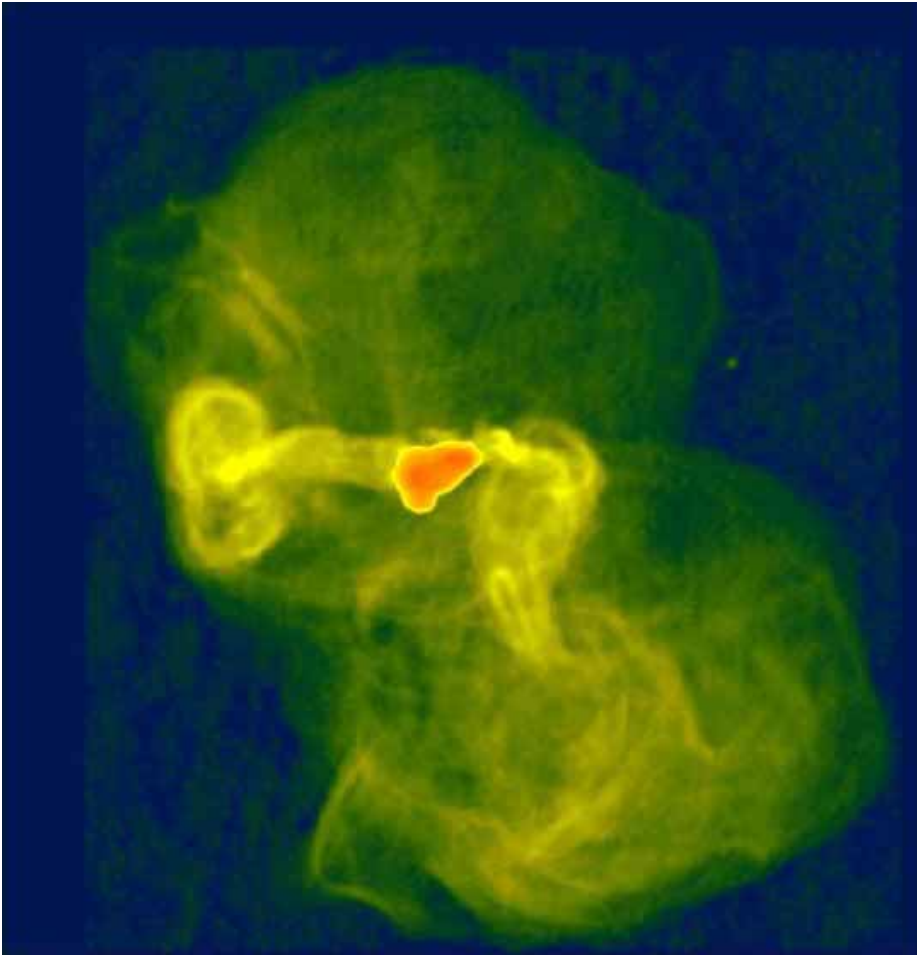


Total intensity

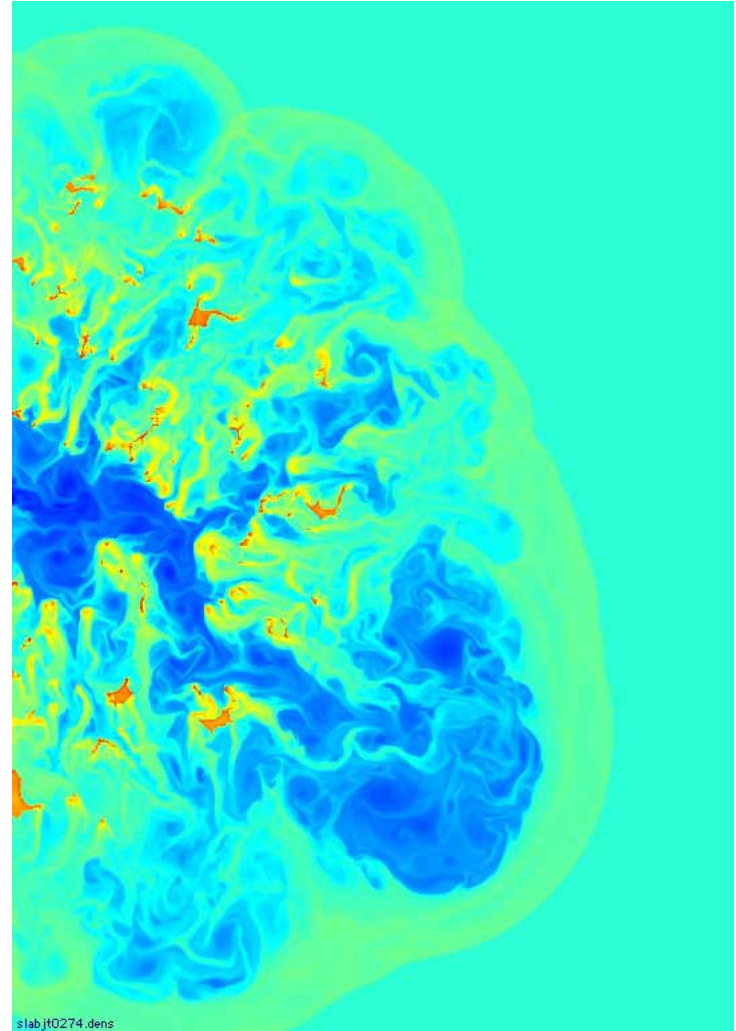


Spectral index

8 Relevance to M87 - interaction with a cooling flow

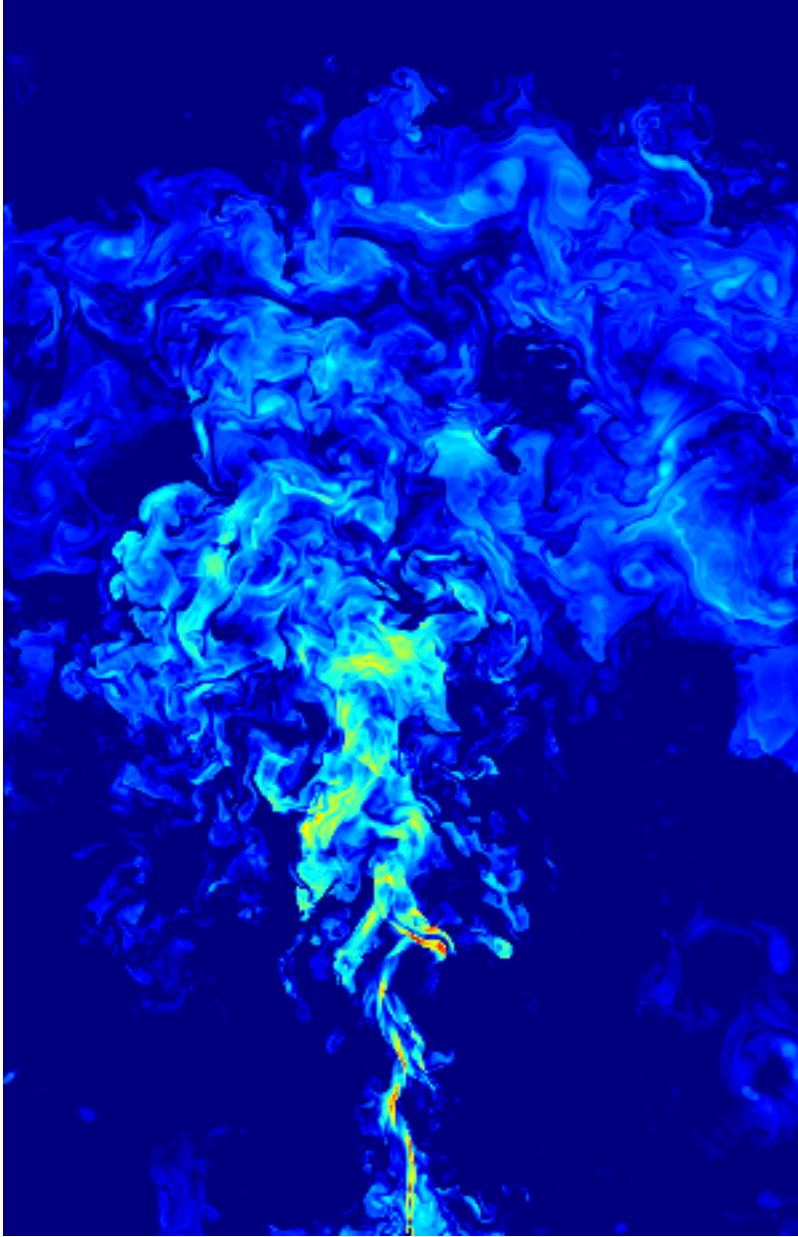


Large scale image of M87 - Owen, Biretta, Kassim & Eilek

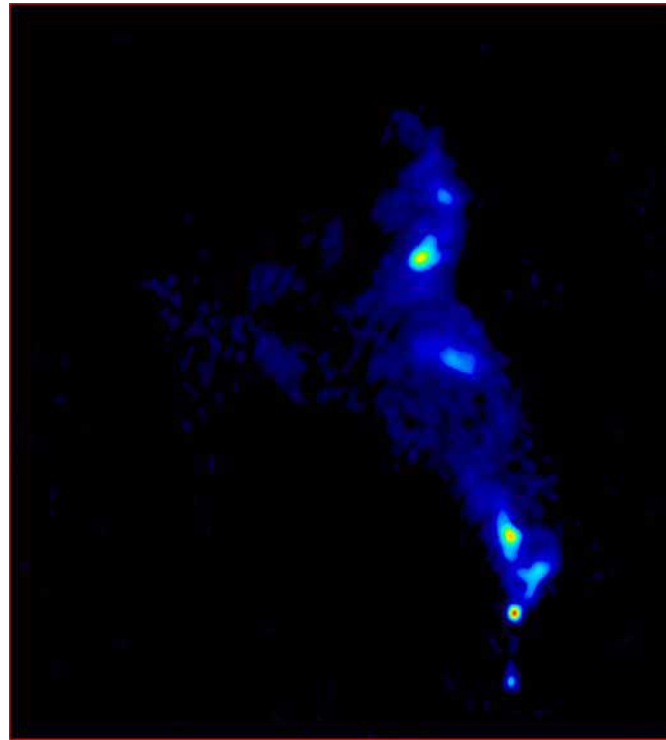


See also Bruggen, Kaiser, Churazov and Ensslin for the additional effect of buoyancy

9 Comparison with 3C48

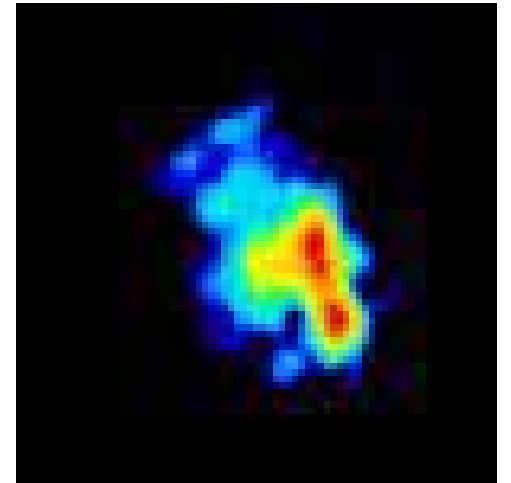


Simulation



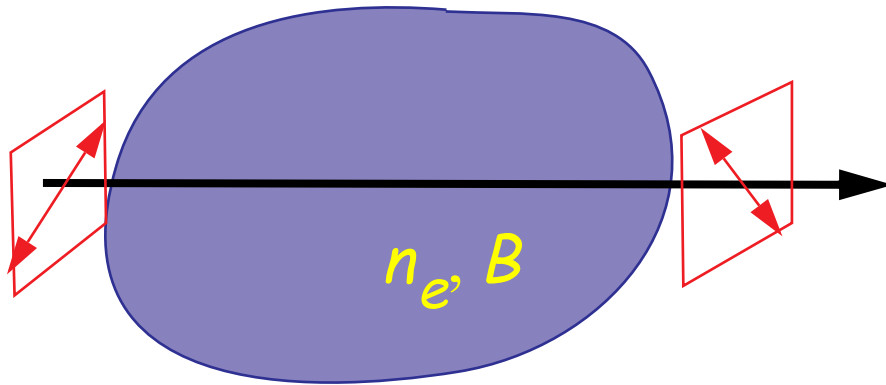
Merlin + VLBA
image of 3C48

Larger scale image
of 3C48 showing
radio halo



10 Observations of rotation measure

The other diagnostic of the interstellar medium that is available from radio observations is rotation measure



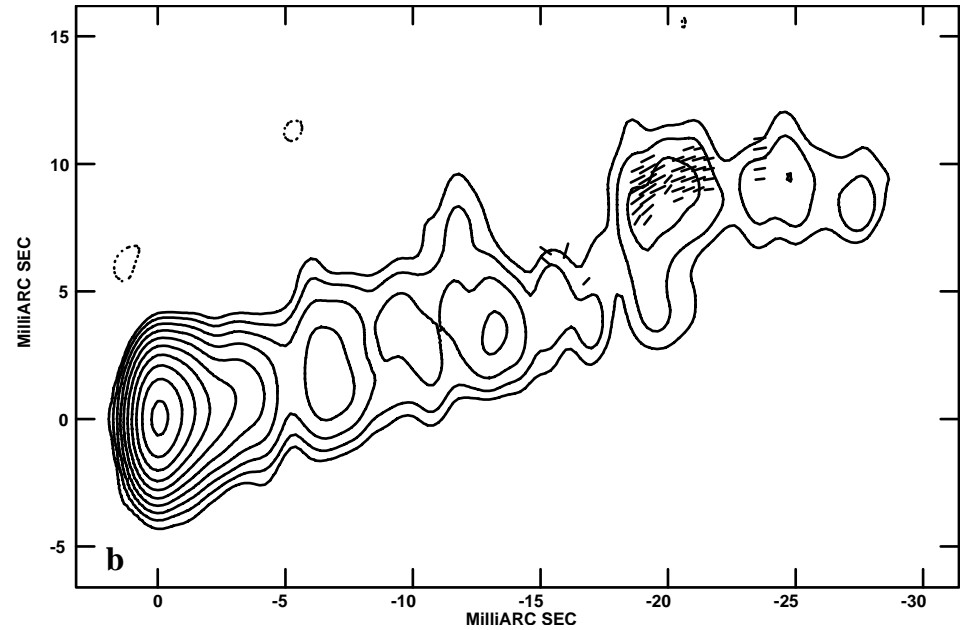
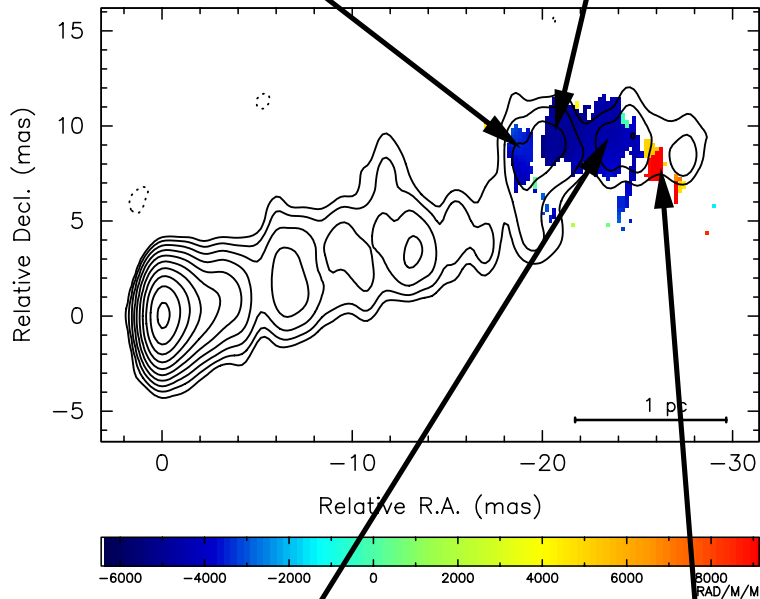
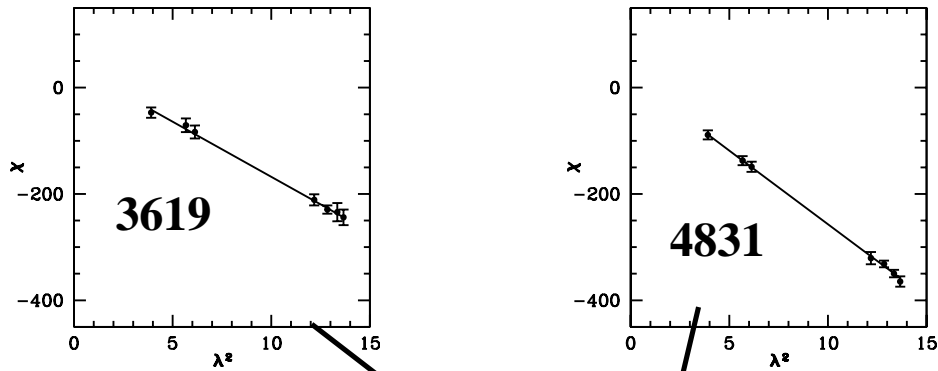
When an electromagnetic wave passes through a magnetoactive plasma (one with $n_e, B \neq 0$) the direction of the linear polarisation is changed by an amount

$$\Delta\chi = \phi\lambda^2$$

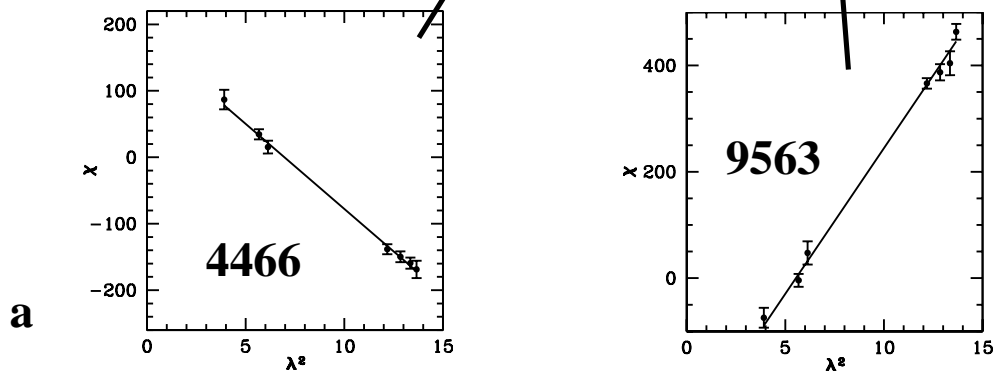
The rotation measure,

$$\phi = \int_{ray} n_e B_{||} dl \quad \text{Units: radians } m^{-2}$$

Rotation measure is a useful indicator of the density and magnetic field in gas associated with the radio source



Jets produce forming and re-forming channels in cloudy medium - relevant for component motion in relativistic VLBI jets



a